Journal of The Electrochemical Society, **151** (9) G612-G617 (2004)
0013-4651/2004/151(9)/G612/6/$7.00 © The Electrochemical Society, Inc.

Physical and Barrier Properties of Amorphous Silicon-Oxycarbide Deposited by PECVD from Octamethylcyclotetrasiloxane

Chiu-Chih Chiang,[a,z] Mao-Chieh Chen,[a,*] Lain-Jong Li,[b] Zhen-Cheng Wu,[b] Syun-Ming Jang,[b] and Mong-Song Liang[b]

[a]*Department of Electronics Engineering, National Chiao-Tung University, Hsinchu 300, Taiwan*
[b]*Taiwan Semiconductor Manufacturing Company, Department of Dielectric and Chemical Mechanical Polishing, Advanced Module Technology Division, Hsinchu, Taiwan*

This work investigates the thermal stability and physical and barrier properties for three species of amorphous silicon-oxycarbide (α-SiCO) dielectric barrier films, deposited by plasma-enhanced chemical vapor deposition (PECVD), to copper (Cu) diffusion using octamethylcyclotetrasiloxane precursor and helium (He) carrier gas with and without oxygen (O_2) reaction gas. The α-SiCO dielectric barrier film deposited by PECVD without O_2 reaction gas exhibits a low *k*-value of 2.8, thermally stable at temperatures up to 550°C, excellent moisture resistance, and superb Cu barrier property until 400°C. With the addition of O_2 reaction gas during the dielectric deposition process, the dielectric constant of the α-SiCO dielectric barrier films increases with increasing flow rate of O_2 reaction gas. Increasing flow rate of O_2 reaction gas during the deposition of the α-SiCO dielectric barrier films also degrades the thermal stability and moisture resistance of the dielectric barrier films. Moreover, the addition of O_2 reaction gas also results in a degraded Cu barrier property of dielectric films.
 [DOI: 10.1149/1.1778169]

Manuscript submitted June 20, 2003; revised manuscript received February 16, 2004. Available electronically August 11, 2004.

As the interconnect resistance-capacitance time delay becomes a dominant factor in determining the performance of ultralarge-scale integrated circuits, the advantages of copper (Cu) metal and low dielectric constant (low-*k*) dielectric materials become more remarkable. Cu has been regarded as the most suitable material to replace aluminum (Al) and its alloys in integrated circuits as the multilevel interconnect material because of its low electrical resistivity and excellent electromigration resistance, and low-*k* dielectric materials can reduce the signal propagation delay, crosstalk noise between metal lines, and power dissipation of integrated circuits. Although many low-*k* ($k < 3$) dielectric materials have been used as inter- and intralayer dielectrics, high dielectric constant ($k > 7$) silicon nitride is still the primary candidate for the Cu-cap barrier and etching stop layer required in the Cu damascene structure. It is desirable to replace silicon nitride with dielectric materials of lower *k*-value ($k < 5$) to further reduce the effective dielectric constant of the Cu interconnect system. In recent years, amorphous silicon-carbides (α-SiC) and amorphous silicon-nitricarbide (α-SiCN) deposited by plasma-enhanced chemical vapor deposition (PECVD) using organosilicate gases are receiving extensive attention for applications as the Cu-cap barrier and etching stop layer in Cu damascene structures because of their lower *k*-value, better etching selectivity with organosilicate glass, excellent chemical mechanical polishing strength, and superb property as a Cu barrier and passivation layer in terms of electromigration resistance and Cu hillock density.[1,2] There are studies on trimethylsilane-based (3MS) α-SiC and α-SiCN barriers that show *k*-values in the range of 4 to 5,[1-4] whereas the α-SiCO barriers deposited using hexamethyldisiloxane (HMDSO) or trimethoxysilane precursor exhibit a lower *k*-value of 3.9.[5,6] Moreover, it has been reported that the α-SiCO barrier deposited using 3MS precursor and He carrier gas with an addition of O_2 reaction gas exhibits a *k*-value of 3.3.[7] In this work, we investigate the thermal stability and physical and barrier properties for three species of α-SiCO dielectric barrier films, with dielectric constants between 2.8 and 6.3, deposited using octamethylcyclotetrasiloxane (OMCTS) precursor and He carrier gas with and without O_2 reaction gas.

Experimental

Three species of α-SiCO dielectric barrier films deposited using OMCTS $\{[(CH_3)_2SiO]_4\}$ precursor and He carrier gas with and without O_2 reaction gas are investigated with respect to their thermal stability and physical and barrier properties. OMCTS is a cyclic structured silicone compound with low water solubility and high vapor pressure. It is a high-safety compound because it converts into SiO_2, H_2O, and CO_2 in the ambient atmosphere. In this study, all of the α-SiCO films were deposited to 50 nm thick on p-type, resistivity 8-12 Ω cm, (100)-oriented Si wafers at 350°C, a total gas pressure of 7 Torr, and a plasma power of 600 W using a parallel-plate PECVD system operated at 13.56 MHz. The flow rate of OMCTS precursor was maintained at 800 standard cubic centimeters per-minute (sccm); while the flow rate of O_2 reaction gas was separately controlled at 0, 200, and 300 sccm, which resulted in three species of α-SiCO films with different elemental compositions. All deposited films were thermally annealed at 400°C for 30 min in N_2 ambient to remove moisture possibly absorbed in the dielectric barrier films prior to the investigation of the films' physical properties or the deposition of electrodes (TaN/Cu or Al) to construct the metal-insulator semiconductor (MIS) capacitor structure. For the construction of TaN/Cu-gated MIS capacitors, a Cu layer 200 nm thick was sputter-deposited on the α-SiCO dielectric barrier film using a dc magnetron sputtering system, followed by a reactive sputter deposition of a 50 nm thick TaN layer on the Cu surface in the same sputtering system without breaking the vacuum. The TaN film served as a passivation layer to prevent the Cu electrode from oxidization during the subsequent high-temperature processes. For comparison, Al electrode control samples were also prepared by depositing a 500 nm thick Al layer directly on the α-SiCO dielectric surfaces using a thermal evaporation system. All metal electrodes with a circular area of 0.84 mm diam were defined by a lift-off process to prevent unexpected deterioration of the dielectric barrier films due to chemical wet etching. For better electrical measurements, a 500 nm thick Al layer was also deposited on the back surface of the Si substrate for all samples. Some of the completed MIS samples were thermally annealed at 400°C for 30 min in N_2 ambient. This annealing step eliminates the plasma-induced damage that may have occurred during the sputter deposition of the TaN/Cu electrodes and also provides the driving force for Cu diffusion.

A semiconductor parameter analyzer (HP4145B) was used to measure the dielectric leakage current and provide the bias for the bias-temperature-stress (BTS) test. Secondary-ion mass spectrometry (SIMS) was used to detect the penetration of Cu in the dielectric barrier films. Fourier transform infrared (FTIR) spectroscopy (ASTeX PDS-17 system) was used to analyze the chemical bonding

* Electrochemical Society Active Member.
z E-mail: ccchiang.ee88g@nctu.edu.tw

Table I. Basic data of OMCTS-based α-SiCO dielectric barrier films studied in this work.

Sample ID	SiCO-0	SiCO-2	SiCO-3
O_2 /OMCTS flow rate (sccm/sccm)	0/800	200/800	300/800
FTIR Si—O/Si—C absorbance peak ratio	1.83	5.07	10.52
Refractive index at 633 nm	1.507	1.439	1.434
Electronic dielectric constant	2.27	2.07	2.05
Dielectric constant at 1 MHz	2.78	4.60	6.30
Ionic and dipolar dielectric constant	0.51	2.53	4.25

of the dielectric barrier films. The film thickness and refractive index were measured using a well-calibrated measurement system (n&k analyzer 1200) at 633 nm wavelength, and the *k*-value of the dielectric barrier films was determined by the maximum capacitance of the Al-gated MIS capacitors measured at 1 MHz using a capacitance-voltage (C-V) measurement system (Keithley package 82). The fabricated details of Al-gated MIS capacitors for C-V measurement are described in the previous paragraph.

Results and Discussion

Physical properties and thermal stability.—Table I shows the basic data of the three species of OMCTS-based α-SiCO dielectric barrier films studied in this work. The α-SiCO dielectric barrier films deposited with an O_2 flow rate of 0, 200, and 300 sccm are designated SiCO-0, SiCO-2, and SiCO-3, respectively. The FTIR Si—O (1020 cm^{-1})/Si—C (800 cm^{-1}) absorbance peak ratio increases with increasing flow rate of O_2 reaction gas during the deposition of the α-SiCO dielectric barrier films. However, the refractive

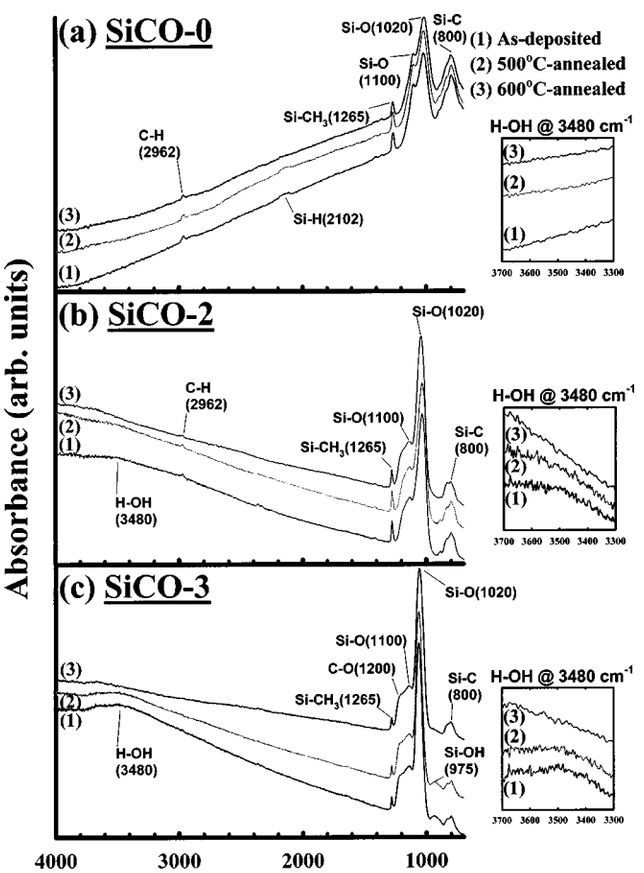

Figure 1. FTIR spectra of (a) SiCO-0, (b) SiCO-2, and (c) SiCO-3 dielectric barrier films with and without thermal anneal.

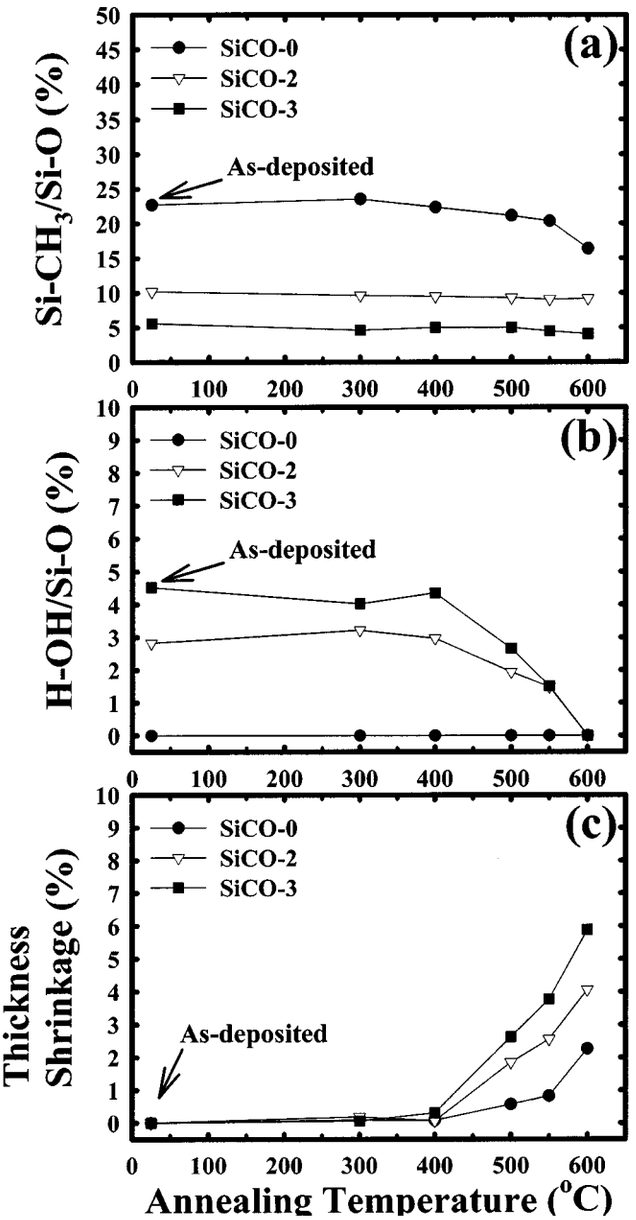

Figure 2. (a) FTIR Si—CH_3 (1265 cm^{-1})/Si—O (1020 cm^{-1}) absorbance peak ratio, (b) FTIR H—OH (3480 cm^{-1})/Si—O (1020 cm^{-1}) absorbance peak ratio, and (c) thickness shrinkage *vs.* annealing temperature for three species of OMCTS-based α-SiCO dielectric barrier films.

index of the α-SiCO dielectric barrier film decreases with the addition of O_2 reaction gas. This result of observation is consistent with those reported in the literature regarding various α-SiCO dielectric films deposited using O_2/3MS, N_2O/HMDSO, O_2/tetramethylsilane (MS), and N_2O/4MS gases.[7-10] The dielectric constant at 1 MHz consists of three components arising from electronic, ionic, and dipolar dielectric constants,[7,8] as shown in Eq. 1

$$k \text{ (at 1 MHz)} = k_e(n^2) + k_{ion} + k_{dipolar} \quad [1]$$

The electronic contribution arises from the displacement of the electron shell relative to a nucleus. The ionic contribution comes from the displacement of a charged ion with respect to other ions, and the dipolar contribution arises from the change of orientation for the molecules with a permanent electric dipole moment in an applied

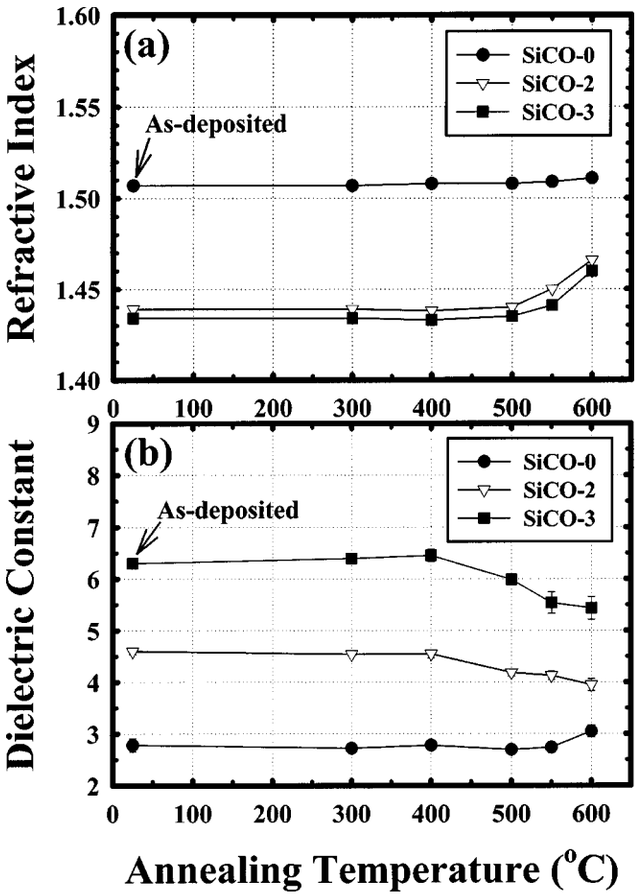

Figure 3. (a) Refractive index and (b) dielectric constant *vs.* annealing temperature for three species of OMCTS-based α-SiCO dielectric barrier films.

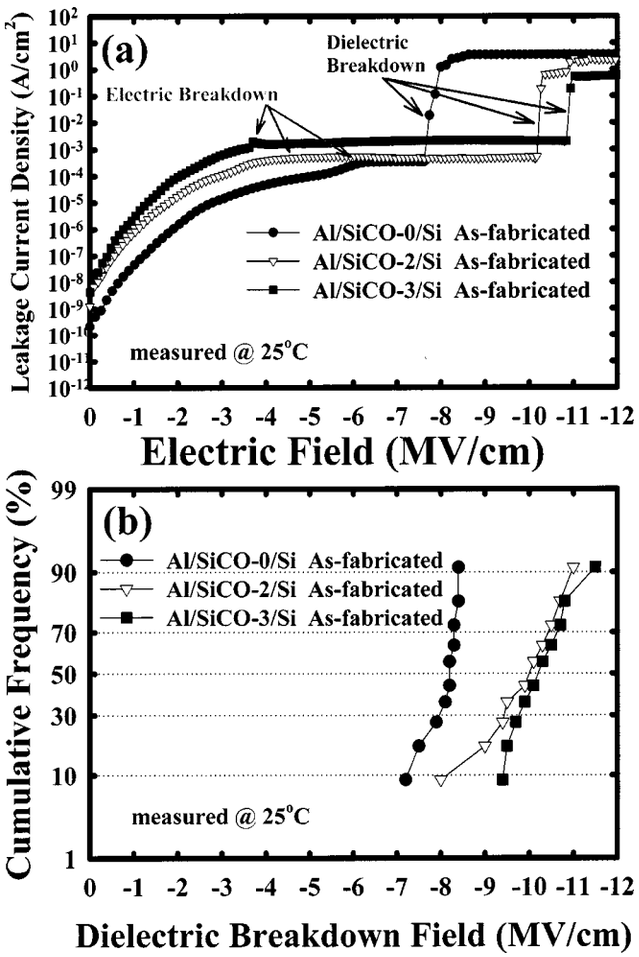

Figure 4. (a) Leakage current density *vs.* electric field and (b) statistical distribution of dielectric breakdown field for as-fabricated Al-gated MIS capacitors.

electric field. Although the electronic dielectric constant, which equals the square of the refractive index,[7,8] decreases with the addition of O_2 reaction gas, the dielectric constant (at 1 MHz) of the α-SiCO dielectric barrier films increases with increasing flow rate of O_2 reaction gas during the film's deposition process. Moreover, the ionic and dipolar dielectric constants, which are obtained by subtracting the electronic dielectric constant from the dielectric constant at 1 MHz,[7,8] increase with increasing flow rate of O_2 reaction gas. The reduction in the electronic dielectric constant of the α-SiCO dielectric barrier films is attributed to an increase in occurrence of the Si—O bond, which is more ionic- and dipolar-polarizable than the Si—C bond.[7,8,11,12] Thus, an α-SiCO film's dielectric constant, which is dominated by electronic polarization, would decrease with increasing incorporation of oxygen.[7] Nevertheless, when the strong ionic and dipolar polarizations of Si—O bonds become predominant in the dielectric constant of an α-SiCO film, the film's dielectric constant is expected to increase with increasing flow rate of oxygen-related reaction gas during the film's deposition process.[8-10] The lower refractive index of the α-SiCO dielectric film implies a lower film density and vice versa,[10] and refractive indexes below 1.46 have been proposed to indicate less dense or porous materials, such as the α-SiCO dielectric films with a porosity of 14-39%.[12,13] It is conceivable that dielectric films with a high density of pores, voids, and other defects tend to contain a high density of bound water because of the film's larger effective surface area,[13-15] *e.g.*, the as-deposited SiCO-2 and SiCO-3 dielectric barrier films whose FTIR spectra reveal a broad peak of the H—OH bond at 3480 cm^{-1}, and a clear Si—OH peak at 975 cm^{-1} observed in the SiCO-3 film, as shown in Fig. 1. Such a susceptibility to moisture may significantly increase the dielectric constant because of the incorporation of H_2O ($k = 80$) and adversely affect the electrical reliability of the dielectric film. The bound moisture (H—OH at 3480 cm^{-1} and Si—OH at 975 cm^{-1}) disappeared completely after the films were thermally annealed at 600°C for 30 min in N_2 ambient. The absorbance of the Si—C (800 cm^{-1}) and Si—CH_3 (1265 cm^{-1}) peaks decrease, whereas that of the Si—O (1020 cm^{-1}) peak increases for the films with increased flow rate of O_2 reaction gas during the films' deposition. Notably, all films show a tiny Si—O shoulder at 1100 cm^{-1}, indicating the existence of the caged Si—O structure in the dielectric films,[10,13] which may result from the OMCTS cyclic precursor. The slight Si—H (2102 cm^{-1}) peak appeared only in the SiCO-0 film, and the small C—H (2962 cm^{-1}) peak was detected only in the SiCO-0 and SiCO-2 films, whereas a distinguishable C—O shoulder at 1200 cm^{-1} was observed only in the SiCO-3 film. Figure 2 shows the FTIR absorbance peak ratios of Si—CH_3 (1265 cm^{-1})/Si—O (1020 cm^{-1}) and H—OH (3480 cm^{-1})/Si—O (1020 cm^{-1}) and the thickness shrinkage for the α-SiCO dielectric barrier films thermally annealed at various temperatures for 30 min in N_2 ambient. Notably, only the SiCO-0 film exhibits chemical outgassing of the CH_3 group above 550°C, whereas only the SiCO-2 and SiCO-3 films exhibit desorption of moisture at temperatures above 400°C. The thickness of all the films remained nearly constant at temperatures up to 400°C. Upon annealing at 550°C, the shrinkage of the SiCO-0 film remained below 1%; however, at 600°C, the film

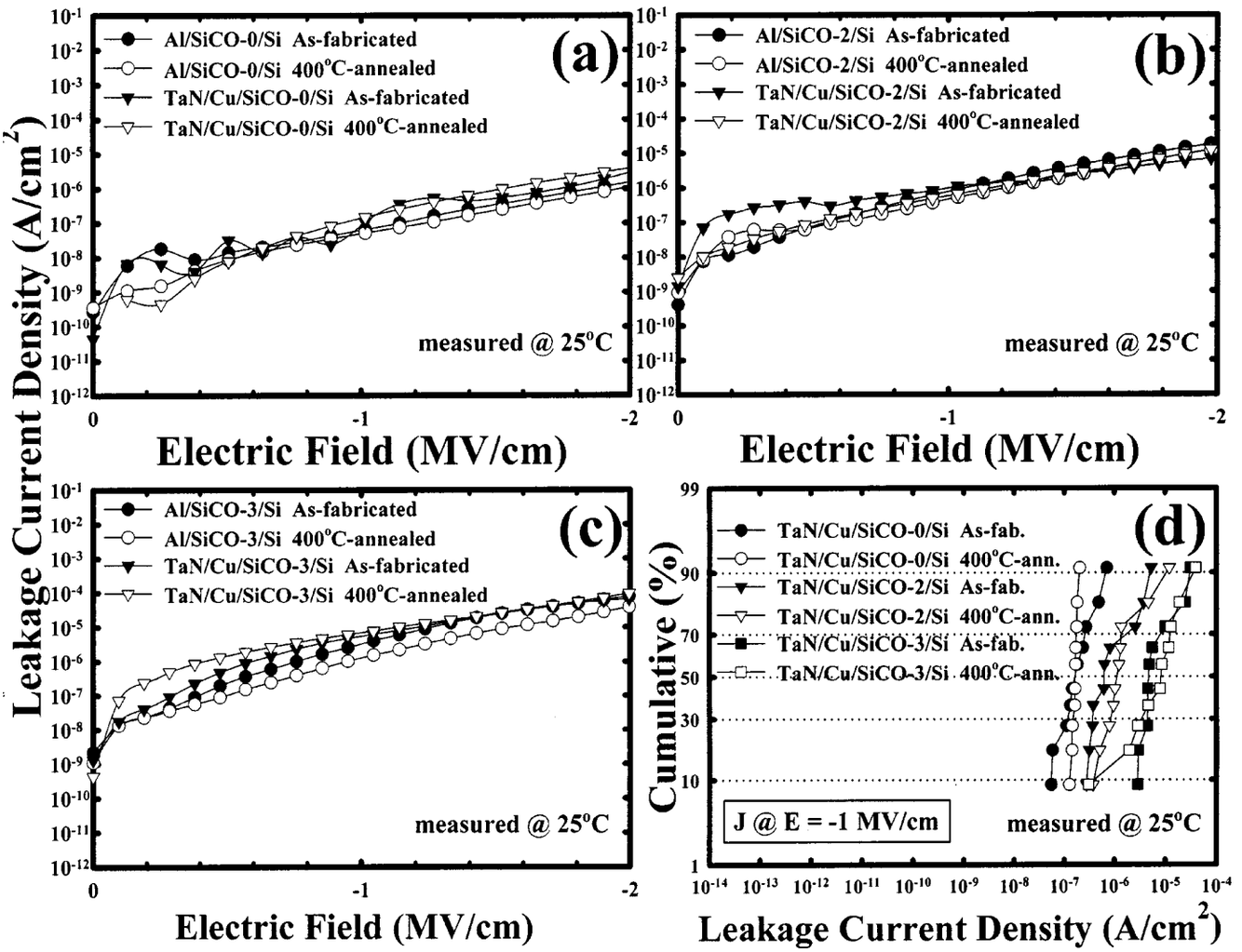

Figure 5. Room temperature leakage current density *vs.* electric field for as-fabricated and 400°C-annealed Al-gated and TaN/Cu-gated MIS capacitors of (a) SiCO-0, (b) SiCO-2, and (c) SiCO-3 dielectric barrier films; (d) statistical distribution of leakage current density for as-fabricated and 400°C-annealed TaN/Cu-gated MIS capacitors.

shrank by more than 2%, presumably due to chemical outgassing, leading to partial removal of the CH_3 group (Fig. 2a). For the SiCO-2 and SiCO-3 films, severer shrinkage (>2%) was observed at and above 550°C, presumably due to the desorption of moisture in the SiCO-2 and SiCO-3 films (Fig. 2b), leading to a denser film structure. The chemical outgassing of the CH_3 group and the desorption of moisture imply the changes in chemical bonding structure and physical microstructure of the dielectric film, resulting in the variation of refractive index and dielectric constant, as shown in Fig. 3. In summary, the OMCTS-based α-SiCO dielectric barrier film deposited without O_2 reaction gas has a thermally stable temperature of 550°C, whereas the films deposited with an addition of O_2 reaction gas have a lower thermal stability temperature, which is about 400°C for the films studied here.

Electrical and barrier properties.—Figure 4 shows the room temperature leakage current density for the as-fabricated Al-gated MIS capacitors of various α-SiCO dielectric barrier films. The measurements were performed with the MIS capacitors biased in the accumulation region. The leakage current characteristics indicate the existence of two breakdown mechanisms: electric breakdown and dielectric breakdown. The electric breakdown, which has been referred to as a soft, quasi-, or nondestructive breakdown and is associated with the creation of a temporary conducting path between the cathode and anode,[16] occurs at an electric field of 4-6 MV/cm. After the electric breakdown, the leakage current reached a saturated value until the occurrence of dielectric breakdown, which has been referred to as a hard, thermal, or destructive breakdown and is associated with the creation of a permanent conducting path between the cathode and anode,[16] at an electric field of 8-11 MV/cm. A similar dual breakdown has been observed elsewhere in the metal-insulator metal capacitors of low-*k* dielectric materials.[17] Notably, the α-SiCO films deposited with the addition of O_2 reaction gas exhibit a higher dielectric breakdown field. This increase of dielectric breakdown field is presumably due to the enhanced Si—O bond, which has a high thermochemical energy.[18] A similar result was observed in the α-SiCO dielectric films deposited using O_2/3MS gases of various flow ratios.[7] On the other hand, the lower electric breakdown fields of the α-SiCO dielectric barrier films deposited with the addition of O_2 reaction gas may result from a larger number of communicating traps[16] such as moisture, voids, pores, or other defects. Figure 5 shows the room temperature leakage current density for the as-fabricated as well as 400°C-annealed (30 min in N_2 ambient) Al-gated and TaN/Cu-gated MIS capacitors of the α-SiCO dielectric barrier films. For each dielectric barrier film, a negligible difference in leakage current was observed between the Al-gated and TaN/Cu-gated MIS capacitors, whether as-fabricated or 400°C-annealed.

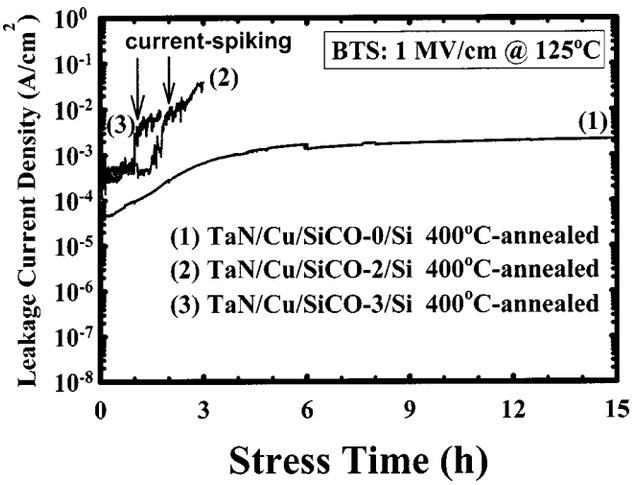

Figure 6. Current transient during BTS test at 125°C with an electric field of 1 MV/cm for TaN/Cu-gated MIS capacitors.

This implies that all the dielectrics are capable of preventing Cu penetration at temperatures up to 400°C. The increased leakage current density for the α-SiCO dielectric barrier films deposited with the addition of O_2 reaction gas (Fig. 5d) may result from the defect and/or moisture induced extra leakage paths.[19] The BTS test was used to further explore the dielectric barrier property of the α-SiCO films using the TaN/Cu-gated MIS capacitor structure. The BTS test was performed at 125°C with an applied electric field of 1 MV/cm on the MIS capacitors that had been annealed at 400°C for 30 min. An N_2 purging was used to prevent oxidation of the Cu electrode and moisture uptake in the dielectric barrier films during the BTS test. Figure 6 shows the leakage current transient during the BTS test. Current-spiking occurred for the SiCO-2 and SiCO-3 dielectric MIS samples after the BTS test for about 2 and 1 h, respectively, whereas the SiCO-0 dielectric MIS sample remained stable up to at least 15 h. Figure 7 shows the SIMS depth profiles of Cu in the TaN/Cu-gated α-SiCO dielectric barrier films after removal of the TaN/Cu electrode. The depth profiles of Cu clearly indicate the penetration of Cu into the SiCO-2 and SiCO-3 dielectric barrier films for the TaN/Cu-gated SiCO-2 and SiCO-3 MIS samples after 3 and 2 h BTS test, respectively. Thus, we may conclude that the current-spiking in the leakage current of the TaN/Cu-gated SiCO-2 and SiCO-3 MIS samples during the BTS test is due to the penetration of Cu into the dielectric barrier films, not the BTS-induced dielectric breakdown. This conclusion is consistent with the results of the BTS test on the Al-gated α-SiCO dielectric MIS samples in which all of them remained stable up to at least 15 h stress (not shown). The inferior barrier property of the α-SiCO dielectric barrier films deposited with the addition of O_2 reaction gas is attributed to the film's microporous Si—O structure.[7] It has been reported that water vapor in the ambient or in the dielectric film markedly enhances the penetration of Cu into the dielectric film, either by hydration-energy induced ionization of metal atoms or by causing deep level electron traps arising from H_2O in the dielectric film.[13,20,21] Moreover, the abundant oxygen in dielectric films possibly enhances the penetration of Cu into the dielectric film by Cu—O reacting.[8,20] Thus, nanopores, moisture, and the abundant oxygen may all enhance the penetration of Cu into the SiCO-2 and SiCO-3 dielectric barrier films and the rapid drift of Cu ions across the barrier layer during the BTS test.

Conclusion

Three species of OMCTS-based α-SiCO dielectric barrier films deposited by PECVD with and without O_2 reaction gas were investigated with respect to their thermal stability and physical and barrier properties. The α-SiCO dielectric barrier film deposited without O_2 reaction gas exhibits a low *k*-value of 2.8, thermally stable at temperatures up to 550°C, excellent moisture resistance, and a superb Cu barrier property until 400°C. With the addition of O_2 reaction gas during the dielectric deposition process, the dielectric constant of the α-SiCO films increases with increasing flow rate of O_2 reaction gas. Increasing flow rate of O_2 reaction gas during the deposition of the α-SiCO films also degrades the thermal stability and moisture resistance of the dielectric barrier films. Moreover, an addition of O_2 reaction gas also results in a degraded Cu barrier property of the dielectric films.

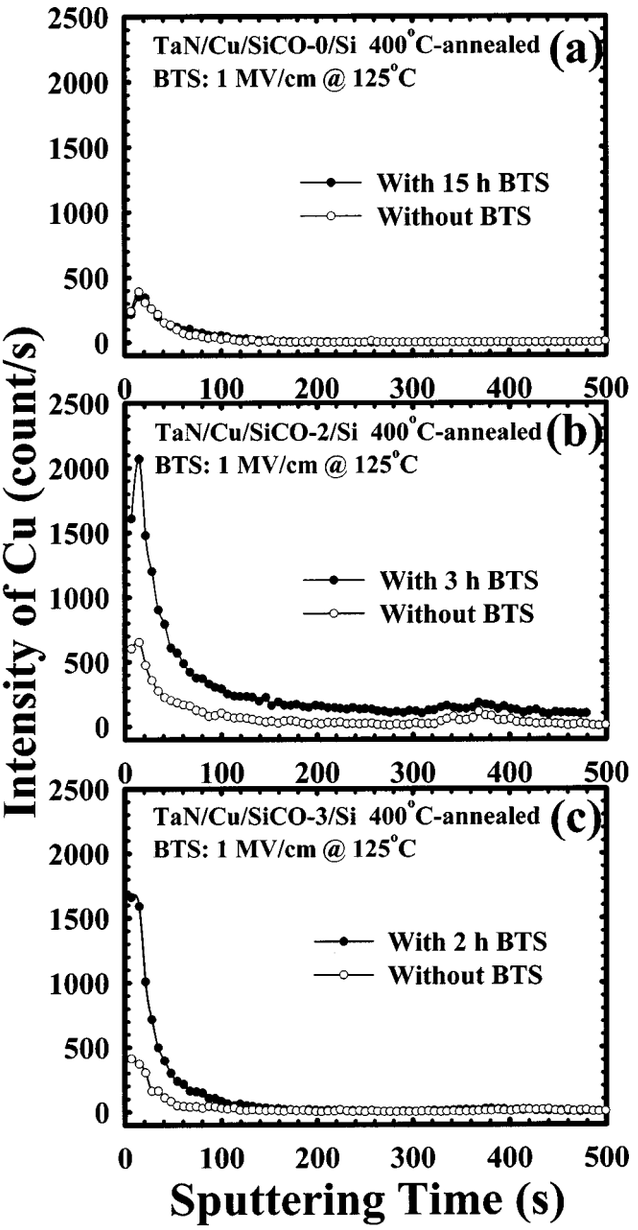

Figure 7. SIMS depth profiles of Cu in (a) SiCO-0, (b) SiCO-2, and (c) SiCO-3 dielectric barrier films of TaN/Cu-gated MIS capacitors with and without BTS test at 125°C with an electric field of 1 MV/cm. The TaN/Cu electrode was removed before the SIMS analysis.

Acknowledgments

The authors express their gratitude to Professor Bing-Yue Tsui of National Chiao-Tung University for his helpful discussion.

National Chiao-Tung University assisted in meeting the publication costs of this article.

References

1. F. Lanckmans, W. D. Gray, B. Brijs, and K. Maex, *Microelectron. Eng.*, **55**, 329 (2001).
2. J. Martin, S. Filipiak, T. Stephens, F. Huang, M. Aminpur, J. Mueller, E. Demircan, L. Zhao, J. Werking, C. Goldberg, S. Park, T. Sparks, and C. Esber, in *Proceedings of the IEEE 2002 International Interconnect Technology Conference*, p. 42 (2002).
3. S. G. Lee, Y. J. Kim, S. P. Lee, H. Y. Oh, S. J. Lee, M. Kim, I. G. Kim, J. H. Kim, H. J. Shin, J. G. Hong, H. D. Lee, and H. K. Kang, *Jpn. J. Appl. Phys., Part 1*, **40**, 2663 (2001).
4. C. C. Chiang, M. C. Chen, Z. C. Wu, L. J. Li, S. M. Jang, C. H. Yu, and M. S. Liang, in *Proceedings of the IEEE 2002 International Interconnect Technology Conference*, p. 200 (2002).
5. T. Ishimaru, Y. Shioya, H. Ikakura, M. Nozawa, Y. Nishimoto, S. Ohgawara, and K. Maeda, in *Proceedings of the IEEE 2001 International Interconnect Technology Conference*, p. 36 (2001).
6. K. I. Takeda, D. Ryuzaki, T. Mine, and K. Hinode, in *Proceedings of the IEEE 2001 International Interconnect Technology Conference*, p. 244 (2001).
7. Y. W. Koh, K. P. Loh, L. Rong, A. T. S. Wee, L. Huang, and J. Sudijono, *J. Appl. Phys.*, **93**, 1241 (2003).
8. T. Ishimaru, Y. Shioya, H. Ikakura, M. Nozawa, S. Ohgawara, T. Ohdaira, R. Suzuki, and K. Maeda, *J. Electrochem. Soc.*, **150**, F83 (2003).
9. A. Grill and V. Patel, *J. Appl. Phys.*, **85**, 3314 (1999).
10. L. M. Han, J. S. Pan, S. M. Chen, N. Balasubramanian, J. Shi, L. S. Wong, and P. D. Foo, *J. Electrochem. Soc.*, **148**, F148 (2001).
11. S. M. Han and E. S. Aydil, *J. Appl. Phys.*, **83**, 2172 (1998).
12. J. Y. Kim, M. S. Hwang, Y. H. Kim, H. J. Kim, and Y. Lee, *J. Appl. Phys.*, **90**, 2469 (2001).
13. Z. C. Wu, Z. W. Shiung, C. C. Chiang, W. H. Wu, M. C. Chen, S. M. Jeng, W. Chang, P. F. Chou, S. M. Jang, C. H. Yu, and M. S. Liang, *J. Electrochem. Soc.*, **148**, F127 (2001).
14. N. Lifshitz and G. Smolinsky, *J. Electrochem. Soc.*, **136**, 2335 (1989).
15. A. Jain, S. Rogojevic, S. V. Nitta, V. Pisupatti, W. N. Gill, P. C. Wayner, Jr., and J. L. Plawsky, *Mater. Res. Soc. Symp. Proc.*, **565**, 29 (1999).
16. J. C. Jackson, Ö. Oralkan, D. J. Dumin, and G. A. Brown, *Microelectron. Reliab.*, **39**, 171 (1999).
17. R. Tsu, J. W. McPherson, and W. R. Mckee, in *Proceedings of the IEEE 2000 International Reliability Physics Symposium*, p. 348 (2000).
18. J. R. Bowser, *Inorganic Chemistry*, p. 401, Brooks/Cole Publishing Co., Pacific Grove, CA (1993).
19. C. G. Shirley and S. C. Maston, in *Proceedings of the IEEE 1990 International Reliability Physics Symposium*, p. 72 (1990).
20. Y. S. Diamand, A. Dedhia, D. Hoffstetter, and W. G. Oldham, *J. Electrochem. Soc.*, **140**, 2427 (1993).
21. J. D. Mcbrayer, R. M. Swanson, and T. W. Sigmon, *J. Electrochem. Soc.*, **133**, 1242 (1986).